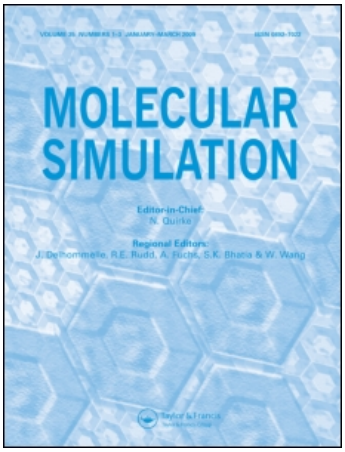

Molecular Simulation
Publication details, including instructions for authors and subscription information:
http://www.informaworld.com/smpp/title~content=t713644482

Interfacial Friction and Collective Diffusion in Nanopores

V. P. Sokhan[a]; N. Quirke[a]
[a] Department of Chemistry, Imperial College London, London, UK

To cite this Article Sokhan, V. P. and Quirke, N.(2004) 'Interfacial Friction and Collective Diffusion in Nanopores', Molecular Simulation, 30: 4, 217 — 224
To link to this Article: DOI: 10.1080/08927020310001659106
URL: http://dx.doi.org/10.1080/08927020310001659106

Molecular Simulation, Vol. 30 (4), 15 April 2004, pp. 217–224

Taylor & Francis
Taylor & Francis Group

Interfacial Friction and Collective Diffusion in Nanopores

V.P. SOKHAN and N. QUIRKE*

Department of Chemistry, Imperial College London, London SW7 2AY, UK

(Received July 2003; In final form August 2003)

A simple Brownian model for the collective dynamics of a fluid confined by rigid walls is described for which the collective velocity autocorrelation function (CVACF) decays exponentially. Using this approach, a new method of calculating the Maxwell velocity slip coefficients from the collective diffusion coefficient, obtained from equilibrium molecular dynamics, is proposed. A comparison of the slip coefficients for a range of fluid densities with the results obtained from the tangential velocity loss of the colliding particles in non-equilibrium simulations show excellent agreement.

Keywords: Collective diffusion; Wall-slip phenomenon; Brownian motion; Interfacial friction; Molecular dynamics; Molecular simulation

INTRODUCTION

A detailed understanding of molecular transport through nanostructured materials is fundamental to the rational design of new materials and devices for nanofluidic solutions to problems involving, for example, high throughput characterisation, analysis and sequencing. Our current understanding of the processes involved in fluid motion in nanoporous solids, in particular the appropriate boundary conditions to use with hydrodynamic models, and the kinetics of fluid inhibition has progressed through advances in both theory [1–3] and simulation [4–6]. However, the precise relation between the transport of fluids in nanopores and the details [2] of the interactions of the fluid with the pore wall remains an open problem.

In solving fluid flow problems the solid is often considered at the continuum level, which simplifies the problem significantly, but requires specifying the boundary conditions. The standard hydrodynamic boundary condition used on a macroscopic scale, the so-called non-slip or stick boundary condition, cannot be simply transferred to nanoscale dimensions. The no-slip boundary condition implies that the fluid velocity at the solid–fluid interface is zero, but recent experimental and simulation work clearly shows that in many cases slip occurs at the pore wall [5, 7–10]. The slip can be quantified by a slip length, a distance from the interface where the extrapolated streaming velocity profile diminishes to zero. This distance is usually of the order of mean free path of the molecules in the fluid and when the transverse dimensions of the system are of the same order of magnitude, the effects of slippage can no longer be neglected. One of the early attempts to describe theoretically molecular slip is due to Maxwell [11] who characterised the gas–solid interactions with a single accommodation coefficient defining the fraction of molecules diffusely reflected from the wall. Recently, a method of estimating the Maxwell slip coefficient from molecular dynamics simulations was suggested [5] based on the analysis of the temporal velocity profiles of molecules colliding with the wall. The slip coefficient in this method is determined graphically once a collision event has been defined for the system of interest. The values of the Maxwell slip coefficient obtained for fully atomic models of static and dynamic walls can be used with non equilibrium molecular dynamics simulations of idealised smooth continuum wall models [12]. This method has the advantage over the methods based on diffuse or Knudsen's cosine law boundary conditions [13] that it can reproduce the flow conditions for a broad range of solids, not only of the ideally rough surfaces. However, since for the Maxwellian walls momentum accommodation

*Corresponding author. E-mail: n.quirke@imperial.ac.uk

ISSN 0892-7022 print/ISSN 1029-0435 online © 2004 Taylor & Francis Ltd
DOI: 10.1080/08927020310001659106

happens instantaneously during the collision, the slip coefficient need to be rescaled, depending on density, in order to match the conditions at the wall. An alternative method is to implement smooth continuum walls with a friction field. Both approximations have been recently explored in the study of fluid flow through carbon nanotubes [12]. The advantage of such methods is that they are faster to compute and are especially appropriate for large systems. However, they require non equilibrium simulations of the full atomic wall model in order to obtain the necessary parameters.

In this work, we develop a new method of calculating interfacial friction force and Maxwell slip coefficients from equilibrium molecular dynamics (EMD) and use it to study the density dependence of the nanopore boundary condition through the Maxwell slip coefficient. In addition, we compare the values of the slip coefficients obtained from EMD with the corresponding values obtained from the temporal velocity profiles predicted by NEMD using gravity-driven Poiseuille flow.

INTERFACIAL FRICTION

In discussing the transport properties of fluids in porous media, the term diffusion describes two related but distinct phenomena. It is usual to consider the tracer or self diffusion of a tagged molecule in a sea of other molecules. This is a non-dissipative process taking place at equilibrium. In an anisotropic system, such as a pore, diffusion is characterised by the self diffusivity tensor which has in general both longitudinal and transverse components: for our purposes we will consider only the longitudinal component. When there are external forces, either mechanical or thermodynamic, acting on the fluid it responds with collective motion which is characterised by the collective, or Stefan–Maxwell diffusivity. Collective diffusivity describes dissipative process and is related to the transport diffusivity which enters the Fick's law using the Darken equation [2]. As follows from the regression hypothesis, collective diffusion can be cast in terms of the equilibrium properties of the system [14]. It can be written as integral of the velocity autocorrelation function in the same way as the self-diffusivity,

$$D = \lim_{t\to\infty}\int_0^t \mathrm{d}\tau\, C(\tau), \tag{1}$$

where C is either the velocity autocorrelation function of the tagged particle,

$$C_\mathrm{s}(t) = N_\mathrm{f}^{-1}\sum_{i=1}^{N_\mathrm{f}} \langle v_i(t)\, v_i(0)\rangle, \tag{2}$$

or a collective velocity, $u(t) \equiv N_\mathrm{f}^{-1}\sum_i^{N_\mathrm{f}} v_i(t)$, autocorrelation function, defined as

$$C_\mathrm{c}(t) = \langle u(t)\, u(0)\rangle \equiv N_\mathrm{f}^{-2}\sum_{i,j=1}^{N_\mathrm{f}} \langle v_i(t)\, v_j(0)\rangle. \tag{3}$$

Here, v_i is the component of the velocity of ith molecule along the pore axis and the angle brackets denote statistical ensemble averaging. The initial conditions are $C_\mathrm{s}(0) = kT/m$, and $C_\mathrm{c}(0) = kT/M$, $(M = N_\mathrm{f}m)$ as required by the equipartition of energy.

The diffusive motion of the tagged particle of mass m is determined by the viscoelastic properties of the fluid as was shown by Zwanzig and Bixon [15] using the Stokes–Einstein relation, and can be treated as classical Brownian motion in one dimension. In the zero-frequency limit it is described by the generalized Langevin equation [16] for the velocity of Brownian particle, $v(t)$,

$$m\frac{\mathrm{d}v(t)}{\mathrm{d}t} = -\int_0^\infty \mathrm{d}\tau K(\tau)\, v(\tau - t) + \xi(t), \tag{4}$$

where $\xi(t)$ is a stochastic fluctuating force representing the microscopic degrees of freedom of the thermal bath, and the kernel, $K(\tau)$, is the memory function responsible for the deviation of the velocity autocorrelation function from Boltzmann behaviour and appearance of the long-range tail found by Alder and Wainwright in 1967 [17,18]. The memory function is related to stochastic force via the fluctuation-dissipation relation,

$$K(t) = (kT)^{-1}\langle \xi(t)\xi(0)\rangle, \tag{5}$$

and can be calculated by molecular dynamics simulation [19]. The algebraic decay of correlations in a fluid is found to be ubiquitous. It is found for the angular velocity autocorrelation functions [20] as well as in confined systems [21] with an exponent in the power law which depends on the number of unconfined dimensions [21].

In certain specific cases the generalized Langevin Eq. (4) simplifies significantly. One of these is the heavy mass limit of the Brownian particle. In this case the environment can be treated adiabatically; the random force reduces to a Markovian noise with zero first moment and with second moment $\langle \xi(\tau)\xi(0)\rangle = 2\eta kT\,\delta(\tau)$, where $\delta(..)$ is the Dirac delta. As follows from Eq. (5), friction in this case has no memory and Eq. (4) becomes the Markovian Langevin equation,

$$m\frac{\mathrm{d}v}{\mathrm{d}t} = -\eta v + \xi, \tag{6}$$

where η is the particle friction coefficient and the time argument is omitted since the nonlocality in time is lost. As a result, the velocity autocorrelation

function of the Brownian particle in this approximation decays exponentially. In recent work exploring the Brownian particle mass and size dependence of the memory function [22] it has been demonstrated, for the example of Lennard–Jones fluid, that the dynamics of the Brownian particle approaches a Boltzmann limit as the mass of the particle increases to infinity. A similar conclusion was reached in a study on a completely different scale; that of the dynamics of a massive black hole in a dense stellar system [23].

There is nothing in the theory of Brownian motion which limits its application to a simple (single interaction site) particle; indeed it is equally applicable to mesoscopic systems with many internal degrees of freedom or to some collective properties [16]. When considering the dynamics of a fluid in a pore the collective motion of the fluid (velocity u) with respect to a stationary pore framework is governed by the same laws as the motion of a finite mass framework with respect to a stationary fluid: in both cases it can be described by Brownian motion. From momentum conservation $m\,\mathrm{d}v/\mathrm{d}t = -M\,\mathrm{d}u/\mathrm{d}t$ and therefore

$$M\frac{\mathrm{d}u}{\mathrm{d}t} = -\eta u + \xi, \tag{7}$$

giving a relation between the self-diffusion of a pore framework, considered as a Brownian particle, and the collective diffusion of the fluid with which it is in contact. Since in our case the pore framework is stationary, or equivalently, of infinite mass, the Brownian motion is Markovian and the Langevin description Eq. (7) is applicable. The collective velocity autocorrelation function is

$$C_{\mathrm{c}}(t) = M^{-1}kT\exp(-t/\tau), \tag{8}$$

where the relaxation time $\tau = M/\eta$ is related to the interfacial friction coefficient η.

The interfacial friction field is related to the tangential momentum accommodation during particle collisions. Within the Maxwell's theory of slip [11] this is characterised by the fraction of molecules, thermalised by the wall, or in the words of Maxwell, "absorbed and then evaporated". Denoting this fraction as α, it is easy to show [24] that the following relation holds

$$\alpha = \frac{N_{\mathrm{f}}}{f_0\tau}, \tag{9}$$

where $f_0 = N_{\mathrm{coll}}/\Delta t$, is the collision frequency in the system. This provides a means to calculate the Maxwell coefficient, α, from the collective velocity autocorrelation function using EMD. In previous work [5] we have described a method of calculating the Maxwell coefficient from NEMD. In what follows we use both methods and compare the results.

SIMULATION RESULTS

Our system consists of N fluid particles confined between two parallel monatomic rigid surfaces placed at $y_{\mathrm{w}} = \pm 2.0\,\mathrm{nm}$ similar to our earlier rare gas–solid model slit pore [5]. The fluid particles interact through a Lennard–Jones (LJ) potential with parameters appropriate for methane, $\varepsilon_{\mathrm{ff}}/k = 148.1\,\mathrm{K}$, and $\sigma_{\mathrm{ff}} = 0.381\,\mathrm{nm}$. The interaction of the fluid particles with the atoms in the wall is also of LJ's form with parameters $\varepsilon_{\mathrm{sf}}/k = 64.39\,\mathrm{K}$, and

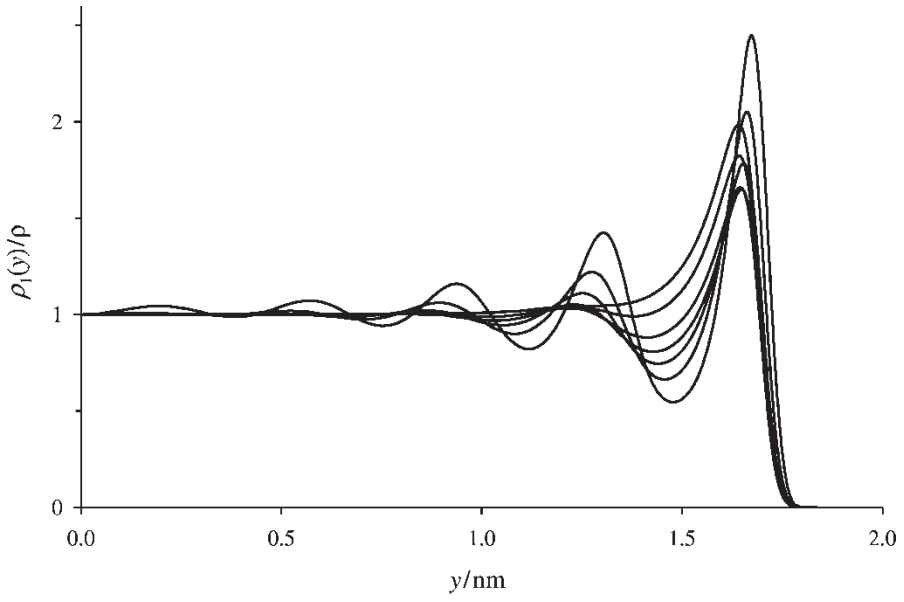

FIGURE 1 Density profiles as a function of the mean density in the pore. The mean density increases for curves read from top to bottom in the first minimum.

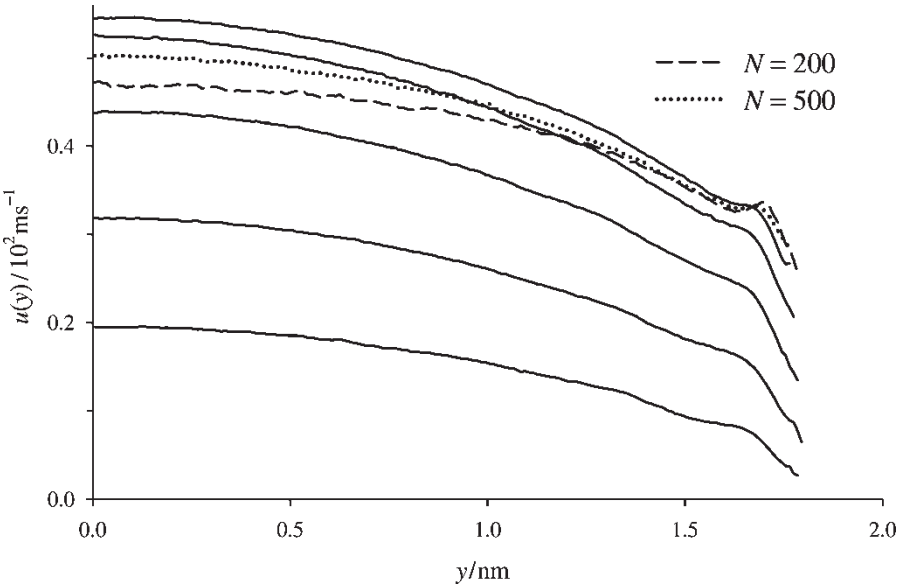

FIGURE 2 Streaming velocity profiles as a function of the mean density in the pore. Apart from the two dashed curves the mean density increases from top to bottom curve. The profiles are symmetrized with respect to the pore axis. The solid wall is at $y = 2.0$ nm.

$\sigma_{sf} = 0.3605$ nm. These parameters were obtained using the Lorentz–Berthelot combining rules with parameters typical for carbon. The dimension of the system in the x and z directions is 7.688 nm. Each of the bounding surfaces consists of 450 atoms, making the reduced surface density of the solid $\rho_s\sigma_{ff}^2 = 1.105$. The fluid is in equilibrium with a thermostat at a supercritical temperature of 300 K.

We considered systems of increasing mean density with N of 200, 500, 1000, 1500, 2000, 2500 and 3032 particles which spans the range from a typical gas density to high liquid density at a normal pressure of 76.8 MPa. The equations of motion were integrated using a velocity Verlet algorithm [25] with timestep of 0.01 ps and the system trajectory was constrained to an isokinetic surface using a Gaussian thermostat. In our calculations we used the DL_POLY code† [26] modified as appropriate for the systems of interest.

For each density two parallel simulations were performed: an EMD at microcanonical conditions and a gravity-driven NEMD with the acceleration due to the external force set to 2×10^{12} ms^{-2}. The non-equilibrium steady state under these conditions is well within the Newtonian flow regime [5]. The integration time is between 0.1 μs for upper density and 0.8 μs for lower density to produce data of comparable statistical accuracy. At least 10 ns equilibration was used in NEMD to let the streaming profiles to settle down.

The density profiles normalized to the mean density in the pore are shown in Fig. 1. They were symmetrized with respect to the symmetry plane of the system, $y = 0$. The density profiles obtained in EMD and NEMD are indistinguishable, and therefore at each density a common plot is shown. The mean density increases from top to bottom (at the position of the first minimum). As the density increases the distance from the wall of the second maximum monotonically decreases, as expected for a compressible fluid. However, the position of the first monolayer does not change appreciably for the first five curves. Only for the last two is it shifted towards the wall, indicating that the surface corrugation, and therefore, the interfacial friction should depend on pressure at these densities.

The streaming velocity profiles obtained in the NEMD simulation are collected in Fig. 2. Apart from two lower densities (for 200 and 500 fluid molecules), denoted on the figure with dashed and dotted lines respectively, the streaming velocity in the middle of the pore decreases monotonically with density. All profiles deviate from a parabolic shape within $1\sigma_{ff}$ from the wall and at the lowest two densities there are regions with positive $\partial u/\partial y$. Applying the linear relation between shear stress and shear viscosity would give a diverging shear viscosity. Other profiles show a shoulder in the same region. The decreasing velocity gradient reflects the local increase in shear viscosity and a comparison with the density profiles (see Fig. 1) shows that this region corresponds to the dense first monolayer of adsorbed fluid‡. The shear viscosity in this region is different

†DL_POLY is a package of molecular simulation routines written by W. Smith and T. R. Forester, copyright The Council for the Central Laboratory of the Research Councils, Daresbury Laboratory at Daresbury, UK, 1996.

‡The apparently linear velocity profile beyond this region, seen at all simulated densities, is usually associated with Couette rather than Poiseuille flow. A possible explanation is that the dense surface monolayer, driven by the mass of the fluid in the pore, forms a moving boundary that together with the solid surface creates a Couette geometry.

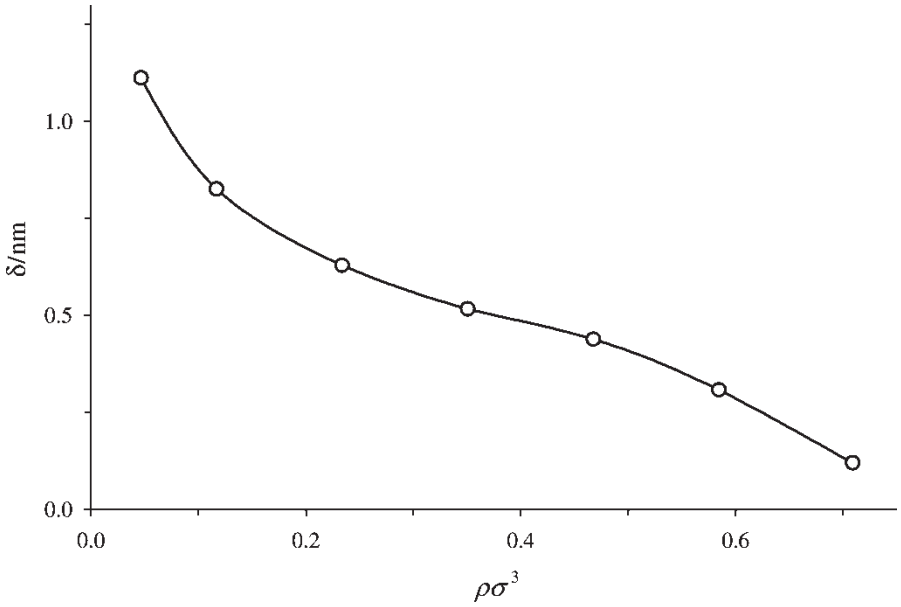

FIGURE 3 Density dependence of the slip length. Circles: results of the NEMD simulation, the line is to guide the eye.

from the rest of the fluid and reflects the *interfacial friction* rather than bulk fluid viscous friction. Outside this region, the shear viscosity appears to be a position-independent quantity which within the calculated density range is described by macroscopic hydrodynamics. By fitting the velocity profile, in the unperturbed region, to a quadratic, a slip length, defined as a position from the wall at which the extrapolated streaming velocity profile decays to zero, was estimated [5].

Figure 3 shows the dependence of the slip length, δ, on the mean density in the pore. The line on the graph is to guide the eye. For the same external driving force the slip length is a decreasing function of density. It diverges at low densities and approaches zero at high density (indicating the validity of no-slip boundary conditions at high density). Slip length is known to depend on the flow rate, see for example the Couette flow experiments of Thompson and Troian [4]. It diverges at high flow rates and this fact should be taken into account when comparing slip lengths at different densities. However, for the rates used in the present work, the rate dependence is weak and will not qualitatively modify our conclusions.

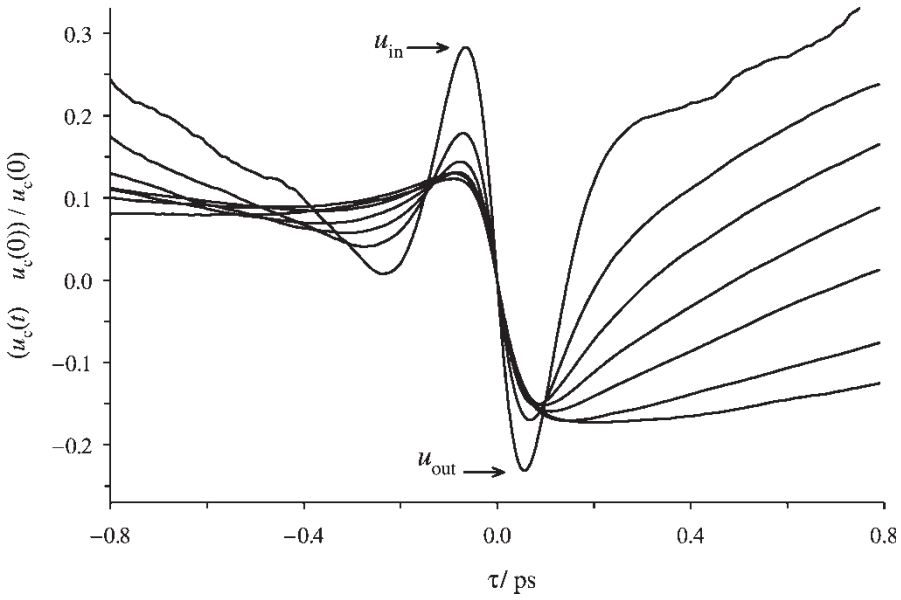

FIGURE 4 Normalized temporal velocity profiles of particles colliding with the wall. The value of the slip velocity has been subtracted from the profiles. The mean density increases from the top to bottom curve in the right central part of the figure.

TABLE I Calculated properties of the system including the collision frequency, normal pressure and the Maxwell coefficient of slip calculated from the temporal velocity profiles and using the relaxation time

$\rho\sigma_{ff}^3$	N	f_0/ps^{-1}	p_{zz}/MPa	α_ν	α_τ
0.0468	200	35.64(2)	1.38	0.265	0.279
0.1169	500	86.77(4)	3.34	0.266	0.264
0.2339	1000	173.12(3)	6.83	0.257	0.252
0.3508	1500	278.61(6)	11.76	0.250	0.253
0.4678	2000	429.28(4)	20.9	0.259	0.261
0.5847	2500	653.40(4)	38.9	0.295	0.296
0.7091	3032	999.57(5)	76.8	0.401	0.407

Figure 4 presents normalized temporal profiles of the streaming velocity of colliding particles. The profiles are centred at the moment of collision with the slip velocity, u_w, identified with the velocity at $\tau = 0$. The mean density in the pore increases progressively for curves from bottom to top in the right hand part of the figure. The Maxwell coefficient of slip is determined by the difference between the molecular velocities before and after the collision [5]. During the collision with the wall particles lose a fraction of the streaming velocity and regain it afterwards through the hydrodynamic drag force induced by the fluid, (note this increases as the fluid density increases). The collision time, which is about 0.1 ps as estimated from the distance between the velocity maximum preceding the collision and minimum after the collision, increases slightly at low densities. Analysis of the temporal depth profiles of the colliding particles shows that the increase of the velocity of the colliding particles before the collision (greater by 17% at high density) is due to acceleration in the external field in the region with lower viscosity (region $y > 1.65$ nm on Fig. 2). It appears to be significantly more pronounced on the figure where the relative velocity is plotted. Slip coefficients, calculated from the graphs using the simple relation $\alpha = 1 - u_{out}/u_{in}$ [5], are collected in Table I, where they are denoted α_τ. They do not change noticeably at low densities and are appreciably different only at two upper densities, where the fluid particles experience a different degree of surface corrugation, as was noted from the inspection of our density profiles in Fig. 1.

The changes in the collective velocity autocorrelation function with fluid density in the pore are shown in Fig. 5. Apart from the two plots corresponding to the higher densities, which decay faster than others, there is no sensible density dependence. The α coefficients estimated from the exponential fit to $C_c(t)$ are denoted in Table I as α_ν and are compared with α_τ in Fig. 6. Comparison of the $C_c(t)$ with $C_s(t)$, shown on the inset to the figure, illustrates the difference in the density dependence. Typical hydrodynamic features, including initial parabolic shape and long-time tail, are absent in the collective autocorrelation function.

The density dependence of the slip coefficients obtained using our two methods is shown in Fig. 6. The standard errors in both cases are of the order of the symbol size. The agreement between two methods at all densities, apart from the lowest, is excellent; the small difference at the lowest calculated density is due to the difficulty in counting

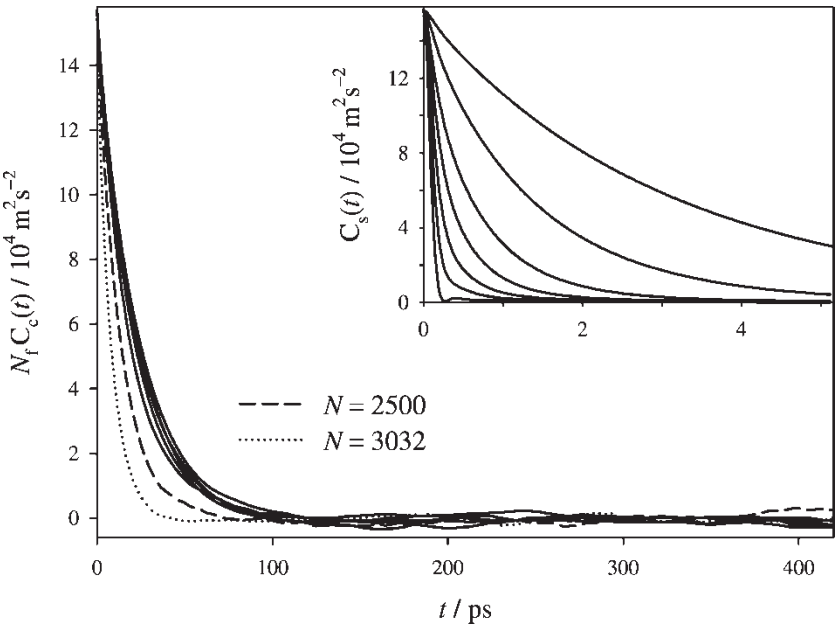

FIGURE 5 Comparison of the collective velocity autocorrelation functions for a range of fluid densities in the pore. On the inset the velocity autocorrelation function of the tagged particle is shown. The mean density increases from the upper to lower curve on the inset.

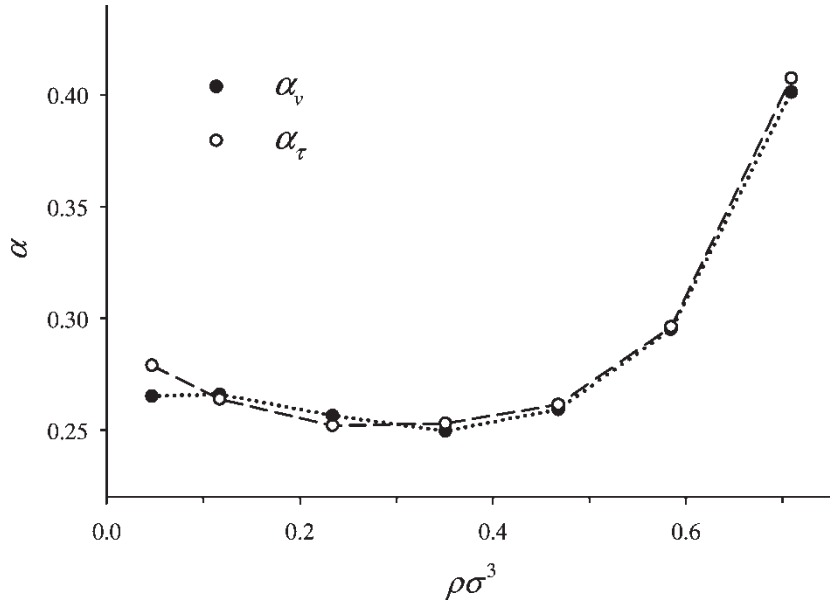

FIGURE 6 A comparison of the α coefficients obtained from the temporal velocity profiles (closed symbols) and from the collective velocity autocorrelation function (open symbols) as a function of density. Lines are to guide the eye.

collision events and we believe that α decreases monotonically for reduced densities up 0.35. A possible explanation of this small decrease in the slip coefficient is the formation of the first adsorbed monolayer which attracts colliding molecules and thus decreases the degree of corrugation "seen" by colliding molecules. The increase in α above the density $\rho\sigma^3 = 0.5$ correlates with the increase in pressure in this region as clear from Fig. 7, where the normal pressure in the pore as a function of density is shown. Summarising, there are two different mechanisms responsible for the density dependence of the α coefficient. One is the normal pressure in the fluid which forces the fluid to explore a progressively higher degree of corrugation of the solid surface; another is the fluid–fluid attraction, which tends to decrease the degree of surface corrugation "seen" by the fluid. The relative importance of these two mechanisms depends on the specific system considered.

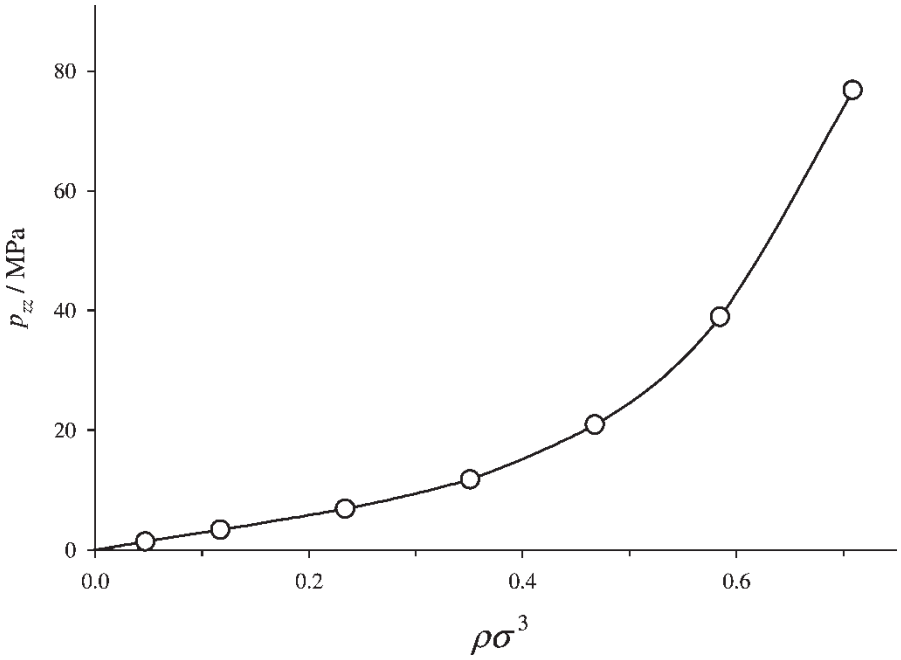

FIGURE 7 Density dependence of the normal pressure in the system.

TABLE II Parameters for the fit of the Maxwell coefficient to pore pressure: $\alpha = \sum_{i=0}^{4} a_i(\ln(p_{zz}/p_0 + 1))^i$

p_0 (MPa)	3.1784
a_0	0.2994
a_1	− 0.1030
a_2	0.0905
a_3	− 0.0409
a_4	0.0082

CONCLUSION

We have shown that the Maxwell slip coefficient can be estimated from the equilibrium properties of the system. Our values are in excellent agreement with the values estimated from an analysis of the wall collision events in NEMD simulations. The calculations show that the slip coefficient is sensitive to the surface corrugation of the solid and is a non-monotonous function of the fluid density. It is, however, approximately constant over a broad range of fluid densities. This result will be useful in devising methods of modelling fluid flow using continuum models for the solid especially for complex geometries where the full atomistic model may require prohibitive amounts of CPU. To model fluid flow at higher liquid densities the coefficient of slip can be scaled to account for changes in the surface corrugation "felt" by colliding particles. For example the expression $\alpha = \sum_{i=0}^{4} a_i(\ln(p_{zz}/p_0 + 1))^i$ with parameters given in Table II fits the data in Figs. 6 and 7.

Acknowledgements

This work is supported in part by the National Physical Laboratory.

References

[1] Vollmer, J. (2002) "Chaos, spatial extension, transport, and non-equilibrium thermodynamics", *Phys. Rep.* **372**, 131.
[2] Kärger, J. and Ruthven, D.M. (1992) *Diffusion in Zeolites and Other Microporous Solids* (Wiley, New York).
[3] Churaev, N.V. (2000) *Liquid and Vapour Flows in Porous Bodies* (Gordon and Breach, Amsterdam).
[4] Thompson, P.A. and Troian, S.M. (1997) "A general boundary condition for liquid flow at solid surfaces", *Nature* **389**, 360.
[5] Sokhan, V.P., Nicholson, D. and Quirke, N. (2001) "Fluid flow in nanopores: an examination of hydrodynamic boundary conditions", *J. Chem. Phys.* **115**, 3878.
[6] Supple, S. and Quirke, N. (2003) "Rapid inhibition of fluids in carbon nanotubes", *Phys. Rev. Lett.* **90**, 214501.
[7] Baudry, J., Charlaix, E., Tonck, A. and Mazuyer, D. (2001) "Experimental evidence for a large slip effect at a nonwetting fluid–solid interface", *Langmuir* **17**, 5232.
[8] Cheng, J.-T. and Giordano, N. (2002) "Fluid flow through nanometer-scale channels", *Phys. Rev. E* **65**, 031206.
[9] Hervet, H. and Léger, L. (2003) "Flow with slip at the wall: from simple to complex fluids", *C.R. Physique* **4**, 241.
[10] Barrat, J.-L. and Bocquet, L. (1999) "Influence of wetting properties on hydrodynamic boundary conditions at a fluid/solid interface", *Faraday Discuss.* **112**, 119.
[11] Maxwell, J.C. (1879) "On stresses in rarified gases arising from inequalities of temperature", *Philos. Trans. R. Soc. Lond.* **170**, 231, reprinted in (1890) *The Scientific Papers of James Clerk Maxwell* (Cambridge University Press, Cambridge) Vol. **2**, p.703.
[12] Sokhan, V.P., Nicholson, D. and Quirke, N. (2002) "Fluid flow in nanopores: accurate boundary conditions for carbon nanotubes", *J. Chem. Phys.* **117**, 8531.
[13] Nicholson, D. and Travis, K. (2000) "Molecular simulation of transport in a single micropore", In: Kanellopoulos, N.K., ed, *Recent Advances in Gas Separation by Microporous Membranes* (Elsevier, Amsterdam), pp 257–296.
[14] Maginn, E.J., Bell, A.T. and Theodorou, D.N. (1993) "Transport diffusivity of methane in silicalite from equilibrium and nonequilibrium simulations", *J. Phys. Chem.* **97**, 4173.
[15] Zwanzig, R. and Bixon, M. (1970) "Hydrodynamic theory of the velocity correlation function", *Phys. Rev. A* **2**, 2005.
[16] Zwanzig, R. (2002) *Nonequilibrium Statistical Mechanics* (Oxford University Press, Oxford).
[17] Alder, B.J. and Wainwright, T.E. (1967) "Velocity autocorrelations for hard spheres", *Phys. Rev. Lett.* **18**, 988.
[18] Alder, B.J. and Wainwright, T.E. (1970) "Decay of the velocity autocorrelation function", *Phys. Rev. A* **1**, 18.
[19] Kneller, G.R. and Hinsen, K. (2001) "Computing memory functions from molecular dynamics simulations", *J. Chem. Phys.* **115**, 11097.
[20] Aliwadi, N.K. and Berne, B.J. (1971) "Cooperative phenomena and the decay of the angular momentum correlation function at long times", *J. Chem. Phys.* **54**, 3569.
[21] Hagen, M.H.J., Pagonabarraga, I., Lowe, C.P. and Frenkel, D. (1997) "Algebraic decay of velocity fluctuations in a confined fluid", *Phys. Rev. Lett.* **78**, 3785.
[22] Kneller, G.R., Hinsen, K. and Sutman, G. (2003) "Mass and size dependence on the memory function of tracer particles", *J. Chem. Phys.* **118**, 5283.
[23] Chatterjee, P., Hernquist, L. and Loeb, A. (2002) "Dynamics of a massive black hole at the center of a dense stellar system", *Astrophys. J.* **572**, 371.
[24] Sokhan, V.P., Nicholson, D. and Quirke, N. (2004) "Transport properties of nitrogen in single walled carbon nanotubes", *J. Chem. Phys.* **120**, 3800.
[25] Allen, M.P. and Tildesley, D.J. (1987) *Computer Simulations of Liquids* (Clarendon Press, Oxford).
[26] Smith, W., Yong, C.W. and Rodger, P.M. (2002) "DL_POLY: application to molecular simulation", *Mol. Sim.* **28**, 385.